

Gas-Cold-Dark-Matter (GCDM) Model of Universal Density Reduction

[Martin Reid Johnson](#)

Trinapco, Inc., 1101 57th Avenue, Oakland, CA 94621 USA

Revision date: September 5, 2023

Abstract: Most of the Universe's baryon mass lies in the intergalactic medium, is unaccreted, and can be treated as an ideal monatomic gas with a uniform comoving density. The thermal loss of such a gas is herein shown to partition into one-third gravity gain and two-thirds entropic gain. The entropic gain of an unbound gas with uniform comoving density is differentially expressed as instant pressure. This instant pressure is proposed as the principal cause of the Hubble parameter. Using gas laws, a three-term expression of the gas's Hubble parameter can be derived from estimated present-day energy density values, which are extrapolated to the time of last scattering, when baryon content was all unaccreted atoms having a uniform comoving density. This "GCDM thermal model" gives an exclusive dependence of the Hubble parameter on baryon mass density. The Λ CDM model is similarly covariant but uses total energy as the central variable instead of baryon mass. Instant pressure at last scatter gives a Hubble parameter that is 25% larger than the value found from baryon acoustic oscillation calculations, which rely on Λ CDM's Friedmann and fluid equations as accurate. These two equations appear to be inaccurate for that time period. Relativistic energy at last scatter gave increased instant pressure, as it made the baryons more dense. These two models' opposing predictions of the effect of relativistic energy density on the Hubble parameter is proposed as the cause of the Hubble tension. Today, the intergalactic medium consists of a plasma. The plasma's instant pressure is fed by Compton scattering and covariant with photon flux. Much of this pressure doesn't obey the gas laws, as it arises from high-energy suprathreshold electrons. This suprathreshold pressure in the late Universe is expressed within the Λ CDM model by giving Einstein's time-invariant Λ a nonzero value. The effects attributed to Λ are proposed to instead arise from the ratio of suprathreshold to thermal energies in the intergalactic medium. Both the presently held time-invariance of Λ , and the Hubble tension, are proposed to arise from neglect of entropic gain. Entropic gain is not found within the Λ CDM model because the Friedmann and fluid equations which comprise the model are developed isoentropically.

Keywords: dark energy, cosmic background radiation, dark ages, reionisation, first stars, large-scale structure of the Universe, cosmology: theory

e-mail: ceo@trinapco.com. ORCID: [0000-0002-5096-3206](https://orcid.org/0000-0002-5096-3206)

1 INTRODUCTION

After Arno Penzias and Robert Wilson's discovery [1] of the cosmic microwave background, or CMB, unanimous consensus rapidly converged around the hot-big-bang concept of the Universe's origin. Consensus converged more slowly around the Λ CDM model [2] as the most empirically accurate explanation of distant star movement to date. The " Λ " in Λ CDM was first proposed by Albert Einstein (see [3] and references therein) and corresponds to a perceived repulsive field, fully scalar in both time t and space xyz . This concept of Λ is historically entrenched within the community of cosmologists and has been applied to the CMB's miniscule anisotropies to calculate the Hubble constant H_0 . These results differ from conventional distance ladder measurements [4-9]. The CMB methods give $H_0 \approx 68$ km/sec/Mpc and the distance ladder methods give $H_0 \approx 74$ km/sec/Mpc. Improved measurements and changed methodology have only made this "Hubble tension" more obvious. Explanations have been proffered to resolve the Hubble tension [10-20]. Most but not all of these rely on Λ . One alternate, quintessence [21], having a time-dependent scalar field, has been proposed. Quintessence is, like Λ and the Higgs field, held to exist *in vacuo*. Of these three only the Higgs field has an experimentally consistent *in vacuo* theoretical foundation, and to date neither Λ nor quintessence have been shown to have a clearly defined, energy-conservative source. Attempts to treat the second law of thermodynamics within a Λ -containing Universe have arisen in numerous papers, many of which (1,800 and counting) cite an original publication by Erik Verlinde [22]. While Verlinde's proposed entropic "screen" or end state has proven quite popular, it tends to indicate that at some point in time, Universal entropy reaches a final value with no further increase. Inconsistency with the second law remains in such treatments.

The present paper takes an approach to Universal expansion consistent with the second law by treating baryon content as the unbound gas it mostly is, making " Λ " variable in the process. The model that arises from this treatment is called the GCDM model, for gas-cold-dark-matter. The GCDM model gives a repulsive field, but this field bears little theoretical resemblance to a quintessent, Λ , or Higgs field. It's currently plasma kinetic energy, is entropic in Nature, and is covariant with both the density and momentum of unaccreted baryons. We will first review relevant thermodynamic principles. We then examine the classic behavior of a freely expanding gas, and use this behavior to construct the GCDM model at the time of last scattering. We then apply this model to the plasma content of the intergalactic medium in the more recent Universe. Finally, GCDM's and Λ CDM's theoretical foundations are compared in the discussion section.

2 ADIABATIC FREE EXPANSION: THE CENTRAL PREMISE OF THE GCDM MODEL

2.1 The two laws of thermodynamics

The first and second laws of thermodynamics were discovered in the 19th century and fully quantified by the 20th. They've stood the test of time, held inviolate by most scientists and all engineers. The first law, in its broadest definition, says that energy is neither created nor destroyed:

$$dE/dt = 0 \tag{1}$$

Where E is the *total energy*, the sum of all forms of energy in the Universe as a whole and in a sufficiently large proxy sphere, generally accepted as 200 megaparsecs (Mpc) or about 600 million light-years (ly) in observed diameter. A sphere this large is said to be *at scale*.

The second law of thermodynamics has had several descriptions over the years. The broadest of these says that entropy at scale is always increasing and can never be zero:

$$dS/dt > 0 \tag{2}$$

Equation (2) links time t and entropy S . If one assumes an isentropic process then (2) requires that no time shall elapse. Setting $dS = 0$ is a common misconception of (2) among cosmologists at present, discussed in section 5.2.

Equation (2) can't be directly compared to (1) because they have different units. At scale, (2) can be directly compared to (1) by expression as gain E_S :

$$d(E_S)/dt > 0 \quad (3)$$

For a gas:

$$d(E_S) = d(TS) \quad (4)$$

Note that (3) and (4) only describe an unbound *system*. "System" usually means e.g. a sealed or *bound* vessel's contents. In this paper it also refers to constant amounts of gas, and more generally total energy, that isn't bound. It's common in a bound system for $d(TS)/dV < 0$ and $d(S)/dV > 0$ if work is performed. However, for both the system and surroundings combined, (3) is always true. At scale, the system *is* the surroundings. There is no scenario at scale where the entropy of the system is increasing and its entropic energy isn't. The converse applies.

We now examine entropic energy gain on a small scale where gravity can be neglected.

2.2 Bound, equilibrium free expansion

Take a spherical helium balloon, of radius $r_1 = 10$ cm, at a temperature $T = 300\text{K}$ and pressure $P = 1$ atmosphere, and place it in the center of a perfectly rigid, insulated, spherical vacuum chamber of radius $r_2 = 50$ cm. The insulation and rigidity of the chamber means any gas expansion from r_1 to r_2 will be adiabatic. The gas's internal kinetic energy U_i is 100% thermal. Helium is monatomic, so:

$$U_i = \frac{3}{2}PV = \frac{3}{2}nRT = \frac{3MRT}{2\mathcal{K}} \quad (5)$$

Where n is the number of moles of gas, R is the gas constant, and \mathcal{K} is the gas's atomic weight. The U_i in the chamber is the instant sum of its atoms' individual kinetic energies:

$$U_i = \sum_{r=0}^{r_2} \sum_{\theta=0}^{\pi} \sum_{\varphi=0}^{2\pi} \left\{ \frac{1}{2} m [(\mathbf{v} \sin[\theta'])^2 + (\mathbf{v} \cos[\theta'])^2] \right\} \quad (6)$$

Where the tensor \mathbf{v} is the atom's kinetic energy, m is its atomic rest mass, r is its distance from the center, θ is its conic angle of latitude, φ is its angle of longitude, and θ' is the conic angle of \mathbf{v} 's deviance from radial. These are shown in two dimensions in Figure 1. The balloon is an *idle* sphere with a constant r_1 . The void between r_1 and r_2 makes no contribution to U_i as long as the balloon is intact.

We pop the balloon. The thermal energy U_i is temporarily and partly transformed into *radial kinetic energy* E_k :

$$E_k = \sum_{r=0}^{r_2} \sum_{\theta=0}^{\pi} \sum_{\varphi=0}^{2\pi} \sum_{\theta'=0}^{\pi/2} \left\{ \frac{1}{2} m [(\mathbf{v} \cos[\theta'])^2] \right\} - \sum_{r=0}^{r_2} \sum_{\theta=0}^{\pi} \sum_{\varphi=0}^{2\pi} \sum_{\theta'=\pi/2}^{\pi} \left\{ \frac{1}{2} m [(\mathbf{v} \cos[\theta'])^2] \right\} \quad (7)$$

Which is the scalar difference between the outward and inward radial components of the atoms' tensors. For an idle sphere, the inward and outward radials of \mathbf{v} in (7) are equal. We can double (7)'s inward radial and replace the radial expression in (6), giving U'_i :

$$U'_i = \sum_{r=0}^{r_2} \sum_{\theta=0}^{\pi} \sum_{\varphi=0}^{2\pi} \frac{1}{2} m [(\mathbf{v} \sin[\theta'])^2] + 2 \sum_{r=0}^{r_2} \sum_{\theta=0}^{\pi} \sum_{\varphi=0}^{2\pi} \sum_{\theta'=\pi/2}^{\pi} \left\{ \frac{1}{2} m [(\mathbf{v} \cos[\theta'])^2] \right\} \quad (8)$$

Equations (7) and (8) combined give:

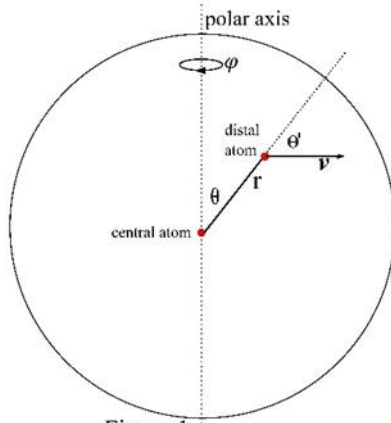


Figure 1.

$$U_k = U_i' + E_k \quad (9)$$

Where U_k is the *total kinetic energy*. When idle, $U_k = U_i' = U_i$. When expanding, $U_k > U_i'$. The instant E_k is the differential gain:

$$E_k = d(E_S) \quad (10)$$

Equation (10) is shown in scalar form. It's more broadly expressed with tensors and links kinetic and entropic energies. Gas gain can be found using (10) without resort to direct calculation of entropy.

Equation (10) is only true for ideal gases. We will use “ E_k ” in several different contexts later. It always describes the kinetic energy of radial movement in some sort of model sphere.

In the special condition of uniform gas density $\rho(t)$, E_k is given as:

$$E_k = P_{V'} dV \quad (11)$$

Where $P_{V'}$ is a physical force, the instant or “entropic” pressure:

$$P_{V'} = \frac{d(E_S)}{dV} \quad (12)$$

Instant pressure $P_{V'}$ is simply covariant P . In the above example, $P_{V'} = P$ only at the instant the balloon is popped. Since ρ is not uniform after the balloon is popped, (11) and (12) don't describe the later behavior of these atoms. However, (9) and (10) remain accurate. Since loss to gravity is negligible, $E_k = (U_k - U_i')$ for the r_2 sphere throughout expansion, which lasts for a second or two. Initially U_i' drops and E_k rises. The atoms quickly bounce off the wall and E_k drops back down. At reequilibrium, $E_k \rightarrow 0$, the terms of (7) again cancel, and U_i is restored: “ $U_i \rightarrow E_k \rightarrow U_i'$ ”. The gain ΔE_S from volume increase is:

$$\Delta E_S = T(S_2 - S_1) = nRT \ln \left(\frac{V_2}{V_1} \right) \quad (13)$$

2.3 Bound, nonequilibrium free expansion

Take that same balloon, put it in the center of a large vacuum chamber ($r_2 = 10^8$ m) and pop it. A helium atom at $T = 300K$ has a root mean square speed $v_{rms} = 1368$ m/s. Those atoms will take about 20 hours to reach the wall of the chamber if their tensor of movement is perfectly radial. As they expand, they stop colliding with each other at any meaningful rate. After that happens, atomic movement is in an unbound regime which is best considered when the atoms have stopped colliding, but haven't hit the wall yet. In this regime, the radial component of each outward atom's speed, or *radial velocity* v_r , is proportional to its distance from the center:

$$v_r/r = H = 1/t \quad (14)$$

The atomic Hubble parameter H is simply expressed by (14). Once the atoms stop colliding, $E_k \approx U_k$ at 300K and $U_i \rightarrow E_k$ almost entirely. The value of E_k remains unchanged until the atoms start to hit the wall. Eventually the atoms bounce off the wall, $E_k \rightarrow U_i$, and the regime slowly ends.

2.4 Unbound, nonequilibrium free expansion

What if there's no boundary? There's no equilibrium to be reached, so for a freely expanding gas, $U_i \rightarrow E_k$ only and there's no $E_k \rightarrow U_i$. One can approach Universal conditions at last scatter by looking only at the comoving core of a popped sphere with initial $r_{core} = 10^{-6} r_{sphere}$. The atoms in that core would be slow, cold, and nearly isodense ($d\rho/dr \approx 0$) with a uniform U_i which obeys (11) and (12). This sort of treatment could be accurate at scales large enough to include gravity. I'm not suggesting that the Universe has finite mass, only that it can be so modeled.

3 CONSTRUCTION OF THE Λ CDM MODEL AT LAST SCATTER, $z = 1089$

Table 1. Values at $z = 0$.

H_0 (km/sec/Mpc)	67.70
H_0 (sec ⁻¹)	2.1938×10^{-18}
ρ_{crit} (kg/m ³)	8.6075×10^{-27}
baryons Ω_b	0.04898
cold dark matter Ω_c	0.26014
relativistic energy Ω_λ	0.000091
dark energy Ω_Λ	0.6908
T_{CMB}	2.6720°K

Notes. H_0 and the Ω values were calculated from table 6 of [24], except for Ω_b , which is $1 - (\Omega_c + \Omega_\lambda + \Omega_\Lambda)$.

The Λ CDM model expresses (1) through a combination of equivalent mass and kinetic energy. We construct the model at last scatter ($z = 1089$) with a finite difference method using the radius r of a sphere as the variable. A spreadsheet is used for the calculations. This is less satisfactory than an analytic derivation, but it does give solace in that expressions herein describe change $U_i \rightarrow U'_i$ with precise instant values. It is only in the partition of ΔU_i between gain (26) and work (25) where error accrues. At last scatter, the BBN estimate for baryons [23] gives a mass proportion of about 75% hydrogen : 25% helium, having a mean atomic weight $\mathcal{K} = 1.24 \times 10^{-3}$ kg/mol. Hydrogen was monatomic and nonrecombinant to diatomic form, absent catalysis through aggregation. The baryon density $\rho_{b(z=1089)}$ was $(\Omega_b \rho_{crit})(1+z)^3 = 5.46 \times 10^{-19}$ kg/m³. This is very low by engineers' standards so we will assume the gas behaved ideally. The

critical mass density ρ_{crit} and the Ω values are given in Table 1. These are CMB values derived by the author from table 6 of [24]. The CMB had almost fully decoupled from the baryons at last scatter by definition, so the baryon temperature T at $z = 1089$ will be set to the extrapolated value $(T_{CMB, z=0})(z + 1) = (2.726K)(1090) = 2971K$.

3.1 The Universe at last scatter had a Euclidean comoving coordinate system

The observed tiny wiggles [24], in the otherwise perfect Boltzmann distribution of the CMB, are telling. There is a metric, η_{slip} , found from the wiggles. It describes variance between Einstein's and Newton's models. At $z = 1089$, if $\eta_{slip} = 1$, then there was no variance, and the atoms in this Universe would have been unaccreted, homogenous, and isotropic, i.e. an isodense gas. The value of η_{slip} was found to be 1.004 ± 0.007 . The text in [24] proclaims that this value of η_{slip} means the models fully converge, so gravitational anisotropy arising from density variance was practically zero. We can then say that at last scatter, atomic movement is accurately expressed with Newtonian momentum tensors in Euclidean space, and (6) - (12) can be applied. The wiggles indicate acoustic oscillation of the baryons. This oscillation gave antinodes of baryon density which grew in magnitude over time and eventually led to gravitational collapse via a process described by the Jeans model [25]. Acoustic oscillation is used by [24] to get an H_A value at last scatter which is then extrapolated to give H_0 today.

3.2 The thermal model at last scatter

The thermal or "dark" model is constructed using monatomic gas expressions found in many introductory engineering textbooks and Wikipedia. Most of the z values in the thermal model ($10 \rightarrow 1089$) cover the dark age [26-27]. The effect of light on the thermal model at $z \geq 10$ is practically nil.

3.2.1 Adiabatic release

Consider a comoving sphere of initial radius r_1 around a single atom of H_1 , at 2971K and $\rho_b = 5.46 \times 10^{-19} \text{ kg/m}^3$. There are similar spheres around all the other atoms. Nonequilibrium conditions besides expansion, e.g. turbulence, acoustic oscillation, etc. will be set aside so that the underlying transformation of conserved energy is more clearly described. There are two competing forces acting on the sphere: Repulsive entropic push, and attractive gravity pull. We are using a finite difference method, so we define an *increment*: $\frac{(r_2-r_1)}{r_1} = \frac{\Delta r_i}{r}$, which must be kept below 10^{-4} for most purposes to minimize the partition error. I use 10^{-9} , as low as the spreadsheet will tolerate. When the gas in the sphere expands, it must do so adiabatically, and there's no void outside the sphere into which free expansion can occur. Under classic bound conditions, the comoving sphere would then have to lose U_i (through work). We postulate that this thermal loss applies in a cosmic setting as well. For monatomic gases the loss is:

$$U_{i_1} - U_{i_2} = -\Delta U_i = \frac{3}{2} P_1 V_1 \left(\left(\frac{V_2}{V_1} \right)^{-\frac{2}{3}} - 1 \right) \quad (15)$$

Where the numeric subscripts refer to the before and after U_i and V values. Volumes V_1 and V_2 are readily found ($4\pi r^3/3$). Thermal pressure P_1 is found from the equation of state for gases, the ideal gas law:

$$P = \frac{\rho RT}{\mathcal{K}} = \frac{MRT}{\mathcal{K}V} = \frac{3MRT}{4\mathcal{K}\pi r^3} \quad (16)$$

If work against gravity is negligible, there is no alternative to free expansion within the sphere that I can find, so the released energy from (15) is, from (9), 100% E_k . Its finite differential value is ΔE_S :

$$E_k = \Delta E_S = \int_{V_1}^{V_2} d(E_S)dV = \int_{V_1}^{V_2} d(TS)dV = \int_{V_1}^{V_2} (TdS + SdT) \approx (S_2 - S_1) \left(T_2 + \frac{1}{2}(T_1 - T_2) \right) \quad (17)$$

Where the subscripts refer to the before and after values on a T-S diagram. Volume increase is strictly local to the sphere. In an infinitely large Universe, it all just gets less dense. The pressure gradient which causes this density decrease is a function of time, not space.

3.2.2 Gravity loss

We now look at the gravitational potential energy U of the sphere:

$$U = \frac{-3GM'^2}{5r} \quad (18)$$

Where G is Newton's constant. The potential energy U must take into account the *total mass* M' , not just M . There's evidence for the existence of cold dark matter (CDM) which is held to be about five times as abundant as baryon mass. Its only interaction with nucleons¹, electrons, or light, is through gravity. CDM is herein treated as a covariant scalar. While it can move relative to accreted baryons like stars, all that occurs within the gravitationally bound network of galaxies known as the "cosmic web", and within Λ CDM, does not affect H . A consistent description of CDM's composition and origin is elusive [28]. Cold dark matter's density evolution is presently treated nonrelativistically; we use this convention. Due to $\eta_{slip} \approx 1$, its density at last scatter can be kept constant with respect to baryon density. Both follow $1/r^3$, as expressed by the *scale factor* a :

$$a = \frac{r}{r_0} = \frac{1}{(z+1)} = \frac{1}{z'} \quad (19)$$

¹ "Nucleon" doesn't include electrons; "Baryon" does. Inclusion of electrons into baryon content is widespread in the literature.

where r_0 is the comoving radius of a sphere today, and z is the cosmic redshift:

$$z = \frac{\lambda_{ob} - \lambda_{em}}{\lambda_{em}} \quad (20)$$

Where λ_{ob} is the observed wavelength of light of known laboratory value, λ_{em} . There's also relativistic CMB energy density $\epsilon_{CMB} = \rho_{CMB}c^2$, which at last scatter fully comprises photon density $\epsilon_\lambda = \rho_\lambda c^2$. It follows $1/r^4$. The effect of these combined densities on H is expressed in the minimum flat-universe Λ CDM model by (21):

$$H_A^2(a) = H_0^2[\Omega_\lambda a^{-4} + \Omega_b a^{-3} + \Omega_c a^{-3} + \Omega_\Lambda] \quad (21)$$

Where H_A is the Λ CDM Hubble parameter, H_0 is today's Hubble constant ($z = 0$), the Ω values are energy density ratios ϵ/ϵ_{crit} at $z = 0$, and the *critical energy density* ϵ_{crit} is:

$$\epsilon_{crit} = \frac{3H^2 c^2}{8\pi G} = \rho_{crit} c^2 \quad (22)$$

The Ω 's in theory always add up to one at any given z , and have identical values when expressed as mass density ratios ρ/ρ_{crit} . In Λ CDM, these contributions to total mass are expressed through a *density multiplier* η :

$$\eta = \frac{\Omega_\lambda a^{-4} + \Omega_b a^{-3} + \Omega_c a^{-3}}{\Omega_b a^{-3}} \quad (23)$$

which gives:

$$M' = M\eta = M \left(\frac{\Omega_\lambda a^{-4} + \Omega_b a^{-3} + \Omega_c a^{-3}}{\Omega_b a^{-3}} \right) \quad (24)$$

Total mass $M' = 6.313M$ at $z = 0$ and increases to $M' = 8.336M$ at $z = 1089$. The reader may be curious as to why Ω_Λ wasn't included in the calculation of M' . It's an artifact of Λ CDM arising from isentropic development and is unrelated to the gravitational effect of mass.

The energy lost to gravity upon expansion of the sphere is:

$$U_r = U_1 - U_2 = \frac{-3GM'^2}{5} \left(\frac{1}{r_1} - \frac{1}{r_2} \right) \quad (25)$$

Where U_1 and U_2 are the before and after gravitational potential energies, respectively.

Atoms can freely expand without colliding. At scale they can perform work without colliding. When the atoms of a model sphere move away from its central atom, they are climbing out of a gravity well caused by the reduced density resulting from their movement, and E_k diminishes accordingly. It is this loss of radial kinetic energy to gravity, not PV work, which is responsible for the "isentropic" portion of thermal loss $-AU_i$.

3.2.3 Release equals loss: the adiabatic sphere

Combining (10), (15), and (25) gives a finite differential expression of thermal loss \rightarrow entropic gain:

$$E_k = \left(\frac{3}{2} \right) P_1 V_1 \left(\left(\frac{V_2}{V_1} \right)^{\frac{2}{3}} - 1 \right) - \frac{3GM'^2}{5} \left(\frac{1}{r_1} - \frac{1}{r_2} \right) \quad (26)$$

A finite expression of conserved total energy is given by (27):

$$E_1 - E_2 = \left[\begin{array}{c} (M_b c^2 + M_e c^2 + M_c c^2 + E_{CMB_1} + U_{i_1} + U_1) - \\ (M_b c^2 + M_e c^2 + M_c c^2 + E_{CMB_2} + \Delta E_{S_{\Delta\lambda}} + U_{i_2} + U_2 + E_k) \end{array} \right] = -\Delta U_i + U_r - E_k = 0 \quad (27)$$

Where E_1 and E_2 are the total energies of the before and after sphere. The CMB gain $\Delta E_{S_{\Delta\lambda}} = E_{CMB_1} - E_{CMB_2}$, discussed in section 5.3.2, is decoupled from E_k at $z < 1089$ and separately expressed. The nucleon rest mass M_b , electron mass M_e , and CDM mass M_c are unchanged at last scatter so their rest energies Mc^2 cancel. Thermal energy U_i is nonrelativistic at 2971K so special effects are negligible and the gas laws are presumed accurate.

When $E_k = 0$ we get an *adiabatic sphere*. Energy is conserved within; it obeys (1). The radius r_e is its adiabatic radius or *endpoint*, found by convergence of r around $-AU_i/U_r = 1$. If we use the value $H_0 = 67.70$ km/sec/Mpc, then at last scatter, $r_e = 9.691 \times 10^{16}$ m (about 10 ly). The sphere's imaginary boundary is its *adiabatic surface*. In today's variegated Universe, the adiabatic surface around a central atom isn't always spherical due to density variance and anisotropic stress near the cosmic web. In these regions E_k must be expressed with tensors. Deep in the IGM the surfaces are near spherical. At last scatter, it's all spheres.

For an adiabatic sphere, the postulate connecting classic to cosmic gas behavior is clearly seen. The thermal loss in the sphere just balances gravity, like a piston's expansion just holding up a weight. The postulate holds for lesser, *medium* spheres, where $E_k > 0$ and thermal loss is partitioned into potential and entropic gain. These medium spheres aren't adiabatic since kinetic energy is escaping from them.

Spheres larger than adiabatic result in gravitational contraction. Although quite interesting, treatment of these *large spheres* as a description of gravitational collapse lies outside the scope of the present paper.

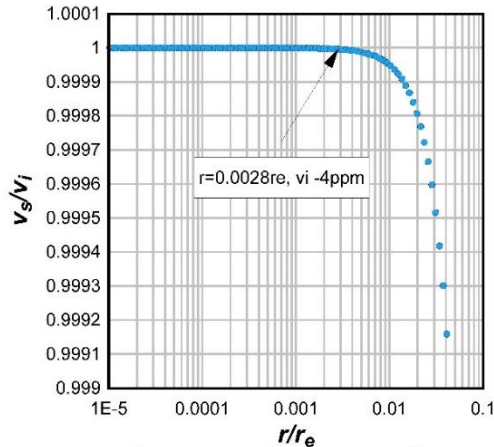


Figure 2. Small sphere cutoff

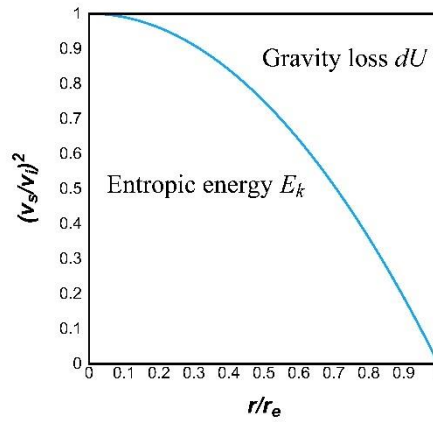


Figure 3. Thermal loss in the adiabatic sphere

3.2.4 The thermal equation, $H_G = Kv_i/r_e$

The adiabatic sphere contains medium spheres which all have $E_k > 0$. To find $d(r_e)/dt = v$, we have to figure out how fast these medium spheres are expanding (28)-(37), and add up their combined radial speeds (38).

The finite differential E_k of a medium sphere gives the *increment radial velocity* v'_s :

$$v'_s = \sqrt{\frac{2E_k}{M}} \quad (28)$$

The term v'_s is best visualized as each and every atom in the sphere moving away from the center at the same speed. We follow v'_s as a function of r , using a constant $\frac{\Delta r_i}{r} = 10^{-9}$. The *small cutoff radius* $r_c = 0.003r_e$ is important. Below r_c , loss to gravity is negligible and all these *small spheres* have the same E_k/M value to within 5 ppm (Figure 2):

$$\frac{E_k}{M} = \frac{\Delta E}{M} = \frac{dE}{dM} = \frac{dV}{dM} \frac{dE}{dV} = \left(\frac{RT}{\mathcal{K}P}\right) \frac{dE}{dV} = \frac{RT}{\mathcal{K}} \left(\frac{dE}{PdV}\right) = \frac{RT}{\mathcal{K}} \quad (29)$$

For a thermal system $dE = -PdV$ at the instant isentropic limit. The minus sign is omitted. Combining (28) and (29) gives the *initial radial velocity* v_i :

$$v_i = \sqrt{\frac{2RT}{\mathcal{K}}} \quad (30)$$

We can determine if energy is conserved within (30) by examining the partition error (31):

$$\frac{\frac{1}{2}M[(v_{i(T_1)})^2 - (v_{i(T_2)})^2] - \Delta E}{\Delta E} \quad (31)$$

We increment a small sphere ($r_1 = 1 \times 10^{12}$ m) giving P_2 and T_2 . The pressure drop from thermal loss of our gas is given by:

$$P_2 = P_1 \left(\frac{V_2}{V_1}\right)^{-\frac{5}{3}} \quad (32)$$

And the temperature drop by:

$$T_2 = T_1 \left(\frac{P_2}{P_1}\right)^{2/5} \quad (33)$$

Which for (30) gives a large error. Development in (29) uses the ideal gas law (16) and not thermal energy (5). We rearrange (5):

$$\frac{U_i}{M} = \frac{3RT}{2\mathcal{K}} \quad (34)$$

Substituting $\frac{U_i}{M}$ for $\frac{E_k}{M}$ in (28) gives:

$$v_i = \sqrt{\frac{2U_i}{M}} = \sqrt{\frac{3RT}{\mathcal{K}}} = \sqrt{\frac{3(8.3145)(2971)}{(0.00123988)}} = 7731 \text{ m/s} \quad (35)$$

By use of (35) the partition error (31) is only 2×10^{-8} , likely its minimum. Since v_i is the fastest rate at which any sphere can expand, increment of a small sphere should not affect its v_i . This error is:

$$\frac{(v_{i(T_2)} + v'_s) - v_{i(T_1)}}{v_{i(T_1)}} = 4.5 \times 10^{-5} \quad (36)$$

As (29) - (36) indicate, thermal $E = U_i$. Einstein's $E = Mc^2$ isn't thermally variable (27). These E terms are conflated within the fluid equation (74) and discussed in section 5.2.

Now that we have what appears to be a proper value of v_i , I propose the radial velocity v_s of a medium sphere as:

$$v_s = \frac{v'_s}{v'_{s0}} v_i \quad (37)$$

Where v'_{s0} is the constant v'_s at $r < r_c$. Equation (37) gives zero at the endpoint, and v_i for $r < r_c$. My guess is v_s/v'_s is constant for $r_c < r < r_e$.

The radial velocity v of the adiabatic sphere is the sum of its contained shells, plus the small core:

$$v = (v_i) \left(\frac{r_c}{r_e} \right) + \sum_{r_c}^{r_e} \left(\frac{r}{r_e} v_s \right) \quad (38)$$

When normalized as v/v_i vs. r/r_e and numerically integrated, the value v/v_i is $0.79210 = K$. This K shows little change with any of M' , ρ , T , or \mathcal{K} ; it's constant to the 5th decimal place.² For an adiabatic sphere with baryon mass M , $E_k = \frac{1}{2}Mv^2 = \frac{1}{2}KMv^2$. This adiabatic E_k is integral, not differential (26).

A normalized plot, $(v_s/v_i)^2$ vs. (r/r_e) (Figure 3) shows thermal loss distribution within an instant sphere as a function of its radius. Its integral value at $(r/r_e) = 1$ is the *entropic partition* $K_S = d(E_s)/-d(U_i)$, exactly $2/3$.³ Only $1/3$ of released energy $-d(U_i)$ is lost to gravity as dU .

A line of adiabatic spheres, connected at their tangent points, can be constructed in the Euclidean space of last scatter. Anywhere along this line, for any two atoms separated by a distance r , their recession rate v_r is:

$$v_r = K \frac{r}{r_e} v_i \quad (39)$$

Rearrangement of (39) gives the fundamental equation:

$$H_G = K \frac{v_i}{r_e} \quad (40)$$

Where $H_G = v_r/r$ is the Hubble parameter of the thermal model. At last scatter, $H_G = 6.319 \times 10^{-14} \text{ sec}^{-1}$, or $28,804H_0$. The Λ CDM model gives $H_A = 5.045 \times 10^{-14} \text{ sec}^{-1}$, or $22,995H_0$; $H_G/H_A = 1.253$ (125%). These differing results unambiguously distinguish the two models.

Deployment of (40) at varying T from 10K to 50,000K at $z = 1089$, or any other dark z value, gives the same $H_G(z)$ to seven decimal places every time. The thermal model is zero-order in temperature. It's also zero-order in \mathcal{K} . A universe made of xenon atoms (0.131 kg/mole) at the same ρ returns 100.000% of our primordial mix's H_G . The mass density ρ is the only independent variable in the thermal model. This sole dependence of H on ρ means that at $z = 1089$, $H_G/H_0 = 28,804$ for any H_0 the reader may prefer. If we move H_0 from $67.70 \rightarrow 74.40 \text{ Km/sec/Mpc}$, we get at $z = 1089$ $H_G = 6.944 \times 10^{-14} \text{ sec}^{-1}$, again $28,804 H_0$. In contrast, at $z = 1089$ H_A/H_0 is always $22,995$. The Hubble tension arises from these differing H/H_0 values: H_A at last scatter is 33% too low.

² Most calculations used 997 steps of linearly increasing r/r_e , beginning at r_c/r_e and ending with $r/r_e = 0.999999$ or 1 at step 997. Derived K values at a 997-point refinement were invariant to 5 decimal places. A 9970-point plot gave $K = 0.792104$ (9969 steps) and 0.792094 (9970 steps); the value $v/v_i = K = 0.79210$ was selected.

³ A 9,970-point plot of $y = (v_s/v_i)^2$ vs. $x = (r/r_e)$ when numerically integrated gave a curve with third-order coefficients $x_0 = -0.00299999$, $x = 1.0000000$, $x^2 = -1.5 \times 10^{-9}$, and $x^3 = -0.33333333$. Correlation = 1. When cutoff $x = 0.003$ is added to x_0 , $y = 1 - x^3/3 = 2/3$ @ $x = 1$.

4 VARIANCE BETWEEN THE Λ CDM AND GCDM MODELS AT $z < 1089$

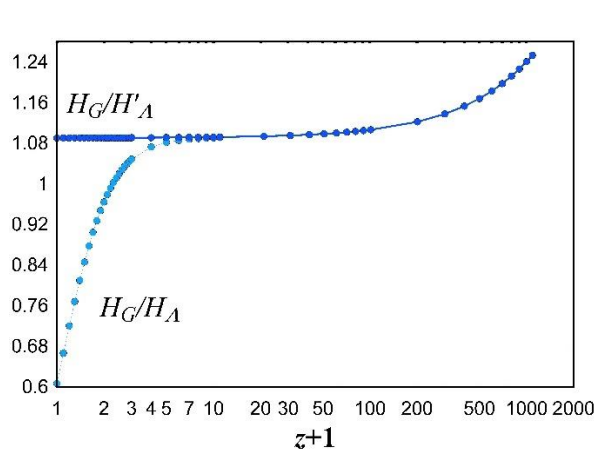


Figure 4. Hubble ratios with and without Ω_Λ

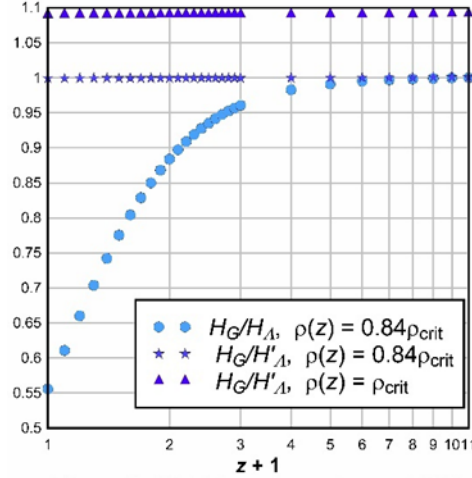


Figure 5. Hubble ratios at low redshift

The GCDM H values at lower z have a complex relationship with both ρ and v_i , occurring in distinct z ranges. The end of one is the start of the other: First, the cosmos partially accreted and formed the cosmic web, affecting H through ρ . Second, light from the web flooded the IGM with free electrons, affecting H through v_i .

4.1 The thermal model at $z = 1089$ to 10: Partition of mass

We interpret the differences between Λ CDM and GCDM for $10 < z < 1089$ as arising from the partition of mass into gravitationally bound and unbound regions of the Universe (the web and IGM respectively). “Dark energy” interferes with accurate visualization of this process at low z values, so we remove the Ω_Λ term in (21):

$$(H'_\Lambda)^2 = (H_0)^2 [\Omega_\lambda a^{-4} + \Omega_b a^{-3} + \Omega_c a^{-3}] \quad (41)$$

Where H'_Λ is the Λ CDM H parameter, without dark energy: A “CDM-only” model. Both H_G (40) and H'_Λ (41) are purely density-dependent functions and we can look at their evolution without interference from extraneous repulsive effects. Their relative behavior is shown in Figures 4-5.

First looking at $z > 10$ (Figure 4), we presume that at $z = 1089$, $H_G = 28,804H_0$ and $\rho = \rho_{crit}$ are both accurate. From $z = 1089 \rightarrow 10$, accretion began at some indeterminate z . An important assumption is made here: Cold dark matter proportionately coaccretes with the baryons and its IGM density remains constant with respect to baryon density. By $z = 10$, the accretion process came to an end and the *mass partition* ρ' has been near-constant ever since (Figure 5):

$$\rho' = \frac{\rho_g}{\rho_b} = 0.840 \pm 0.002 \quad (42)$$

Where ρ_g is the mean gas density: Baryon mass in the IGM alone divided by total volume, web included. Since $\rho_g = 0.84\rho_b$, we may conclude there’s $5\frac{1}{4}$ times as much baryon mass in the IGM which separates the tendrils of the cosmic web as there is in the tendrils themselves, which at present comprise only $\approx 10\%$ of total volume. It’s the 84% of mass in the IGM that’s doing the expanding; the mass in the web is mostly just going along for the ride. A classic analogy would be a bound, adiabatic, and idle small sphere of helium. Some 16% of the helium’s rest mass is then converted to bismuth dust which floats around with the same rest mass. The sphere retains its M , V , and T , but its ρ' drops so its P also drops, by 16%. At scale, accretion similarly reduces $P_{V'}$ and gravity comes into play. In a hypothetical Universe which has 100% accretion, Friedmann kinetics (70) would be accurate and not (40). We

treat this ‘‘Friedmann effect’’ at 16% accretion through ρ' . Such treatment of web mass’s effect on H may be reductive in volume, and sidesteps a proper analysis the web’s contribution to H , but the fit of ρ' with H_G/H'_A is good (Figure 5) and we’ll use ρ' to get thermal values of H when we examine $z < 10$.

The variance of H_G/H_A due to added repulsive energy remains, as shown by the circles in Figure 5. This author has found three additional unresolved issues; doubtless there are others.

4.1.1 The accretion parameter

How did accretion $(1 - \rho')$ evolve during the dark age? An analytic expression $H(z)$ can be derived and used to estimate $\rho'(z)$. In this subsection, $H_0 = 67.70$ km/sec/Mpc is used to get both $H_G(z)$ and $H_A(z)$.

The redshift z_2 can be obtained from any starting value z_1 by changing the increment $\frac{\Delta r_i}{r}$:

$$z_2 = \frac{z_1+1}{\frac{\Delta r_{i+1}}{r}} - 1 \quad (43)$$

The temperature T_z is found from (32) and (33) using (43) to get V_2 . Given $T_{(z'=1090)} = 2971\text{K}$, we find from the spreadsheet that $T_{z'} = T_{(z+1)}$ is exactly:⁴

$$T_{z'} = T'(z')^2 \quad (44)$$

Where the *root temperature* $T' = 0.0025$ is expressed as degrees K. If treated as an abrupt decoupling at $z = 1089$, then at $z = 60$, $T = 9.3\text{K}$; at $z = 10$, $T = 0.3\text{K}$. These are lower than other estimates [29] but since H_G is temperature-independent, dark thermal heating by the CMB doesn’t affect H . We just need the root temperature.

We insert (44) into (35), giving:

$$v_i = \sqrt{\frac{3RT'z'^2}{\mathcal{K}}} \quad (45)$$

The endpoint r_e is adjusted for both T and ρ .

For the T adjustment, the thermal radius change r_{e_2}/r_{e_1} vs. T at constant ρ and \mathcal{K} is found exactly:

$$r_{e_2} = r_{e_1} \sqrt{\frac{T_2}{T_1}} \quad (46)$$

For the ρ adjustment, the thermal radius change r_{e_2}/r_{e_1} vs. ρ at constant T and \mathcal{K} is found exactly:

$$r_{e_2} = r_{e_1} \sqrt{\frac{\rho_1}{\rho_2}} \quad (47)$$

For nonrelativistic mass,

$$\frac{\rho_1}{\rho_2} = \frac{(z'_1)^3}{(z'_2)^3} \quad (48)$$

Combining these gives:

⁴ 210 points from $z' = 1090$ to 10; median $z' = 350$. Found: $T = 2 \times 10^{-9} + 5 \times 10^{-11}(z') + 0.002500631 (z')^2$; correlation = 1.

$$r_{e_2} = r_{e_1} \sqrt{\frac{z_1'}{z_2'}} \quad (49)$$

Inserting (45) and (49) into (40) gives:⁵

$$H_G = K \frac{v_{i_2}}{r_{e_2}} = \frac{K}{r_{e_2}} \sqrt{\frac{3RT'(z_2')^2}{\mathfrak{K}}} = \frac{K}{r_{e_1}} \sqrt{\frac{3RT'(z_2')^3}{\mathfrak{K} z_1'}} \quad (50)$$

At last scatter, $z_1' = 1090$. We adjust for relativistic mass with \mathfrak{m}' :

$$\mathfrak{m}' = \frac{\mathfrak{m}_{z_2'}}{\mathfrak{m}_{z_1'}} \quad (51)$$

Where $\mathfrak{m}_{z_1'} = 8.336$ is the multiplier at last scatter. A linear dependence of H on \mathfrak{m}' is found from the spreadsheet:

$$H_G = \frac{K}{r_{e_1}} \mathfrak{m}' \sqrt{\frac{3RT'(z_2')^3}{\mathfrak{K} z_1'}} \quad (52)$$

When ρ' is set to 1, the deviance of (52) from the manually calculated values of H_G (40) is < 0.1 ppm for all $z = 1089$ to 0. In this ideal case, we only need to calculate r_e at last scatter to get thermal H values at lower z . However, mass accretion is untreated in (52) so a partition term $\rho_{z'}$ must be inserted, from (47) as the square root:

$$H = H_G \sqrt{\rho_{z'}} = \frac{K}{r_{e_1}} \mathfrak{m}' \sqrt{\frac{3RT'(z_2')^3}{\mathfrak{K} z_1'} \rho_{z'}} \quad (53)$$

Rearrangement of (53) gives:

$$\rho_{z'} = H^2 \frac{(r_{e_1})^2}{K^2 (\mathfrak{m}')^2} \frac{\mathfrak{K} z_1'}{3RT'(z_2')^3} \quad (54)$$

For $z > 10$, “dark energy” is minimal ($\Omega_\Lambda < 0.002$), and $\rho_{z'} = \rho'_{(z+1)}$ might be estimable from the H values of any luminous bodies we are fortunate enough to see. This depends on whether or not star formation and accretion are coevolving phenomena. For $z > 10$, if accretion ends before starlight begins, then $\rho' = 0.84$ applies and the value of H/H_Λ will remain close to one. However, if accretion and starlight coevolve, then $H/H_\Lambda > 1$ may be significant enough to measure, and (54) can be applied. For example, the newly found galaxy JADES-GS-z13-0 [30-31] has a spectroscopic redshift of 13.2, so $\Omega_\Lambda = 0.0007$, a minimal dark energy value, and $H'_\Lambda \approx H_\Lambda$. If $\rho' = 0.84$ at this redshift then $H/H_\Lambda = 1.002$, not significant. If $\rho' = 0.9$ then $H/H_\Lambda = 1.036$ which if true ought to be detectable. In a coevolving Universe, observed H/H_Λ differences should get more pronounced at higher z values. This author believes that star formation and accretion do coevolve, and I predict upwardly-trending deviance of H from H_Λ in the $z > 10$ range now accessible from the James Webb telescope. This trend should be observable regardless of which H_0 is chosen. For $H_0 = 67.70$ km/sec/Mpc, the upper limit of H/H_Λ is 1.253, the last-scatter value, which can't be seen since there's no stars at 0% accretion. When more data from Webb comes in, we should be able to follow the progress of accretion through the parameter $(1-\rho')$.

⁵ Use of (44) to get r_{e_2} in (50) indicates that the adiabatic mass M_e isn't constant with U_k , but is instead a roughly colinear function of z' . This is a somewhat counterintuitive result.

4.1.2 Cold dark matter

Cold dark matter can be supposed to have its own U_i which undergoes loss from work dU . Any such loss is discounted by the thermal model: At last scatter, gas does all the work. Consistency with (1) dictates that within Λ CDM, CDM was and is so cold that its U_i , U_k , and E_k are all zero. These unusual premises are questionable and presently inconclusive. In this context the reader may wish to reexamine the rate of accumulation of old neutrinos in the very early Universe, more properly accounting for the irreversible nature of their large entropy of formation, and of their similarly large present-day Compton wavelength.

4.1.3 Are the Friedmann and thermal models analytically equivalent?

The “CDM-only” model (41) and thermal model (40) converge for $z < 10$ if accretion ρ' is included. Their equivalence is likely but unproven. To do so, the effects of CMB mass and “dark energy” must be parsed out. The former of these is low enough to be neglected for $z < 9$ and in any event a simple function of z . “Dark energy” is herein proposed as neither constant nor a directly dependent function of z , and proper resolution of its effects must rely on observed H values.

4.2 The light model, $z = 10$ to 0: Suprathermal energy

None of the above expressions come any closer to explaining the source of the repulsive “dark energy” term Ω_Λ in the Λ CDM model. I propose that suprathermal kinetic energy in the IGM is responsible. It arises mostly from Compton scattering, reliant in turn on photon flux dE_γ/dt . There are partial flux estimates available [32-33] but the process of connecting these and other sources to produce a definitive “light model” is an undertaking of considerable magnitude. The present paper is merely an introduction.

Suprathermal kinetic energy adds pressure to the IGM:

$$P_{V'} = P_{V'_t} + P_{V'_s} \quad (55)$$

Where $P_{V'_t}$ and $P_{V'_s}$ are thermal and suprathermal pressures respectively.

The thermal model (40) has three terms: K , v_i , and r_e . If we want to express suprathermal content within that framework, we need to increase v_i or K , decrease r_e , or some combination. We express v_i (35) as a sum:

$$v_i = \sqrt{\frac{2(U_{i_t} + U_{i_s})}{M}} \quad (56)$$

where U_{i_t} and U_{i_s} are thermal and suprathermal kinetic energies in the adiabatic sphere.

The total nucleon kinetic energy U_b is:

$$U_b = U_{b_t} + U_{b_s} \quad (57)$$

Where U_{b_t} is the thermal value of U_b , and U_{b_s} is cosmic radiation.

The total electron kinetic energy U_β is:

$$U_\beta = U_{\beta_b} + U_{\beta_t} + U_{\beta_s} \quad (58)$$

Where U_{β_b} is the thermal energy of atomically bound electrons, U_{β_t} is the thermal energy of free electrons, and U_{β_s} is their suprathermal energy.

Inserting (57) and (58) into (56) gives:

$$v_i = \sqrt{\frac{2[(U_{b_t} + U_{\beta_b} + U_{\beta_t}) + (U_{b_s} + U_{\beta_s})]}{M}} \quad (59)$$

We neglect cosmic radiation U_{b_s} for now as its omission doesn't substantially affect the logic of the following expressions. This means $U_{b_t} = U_b$, so:

$$v_i = \sqrt{\frac{2(U_b + U_{\beta_b} + U_{\beta_t} + U_{\beta_s})}{M}} \quad (60)$$

We examine the thermal energies U_{β_b} (bound) and U_{β_t} (free). Thermal free electrons are held to behave at very low densities as a monatomic gas. Treatment as such reduces the mean atomic weight \mathcal{K} . The thermal model is independent of both \mathcal{K} and T and dependent only on the mean gas density ρ_g . The result of thermal ionization is thus an increase in both v_i and r_e without affecting H or K . If v_i is doubled, so is r_e , as is the case with pure hydrogen plasma which will serve as our example.

In a thermal system with no ionized H_1 :

$$U_i = U_b + U_{\beta_b} \approx 1.0005U_b \quad (61)$$

so $U_i = U_b$ is reasonably accurate. When H_1 is 100% ionized at e.g. 4000K, the number of gas particles is doubled, the atomic weight halved, and energy equipartitioned: $U_{\beta_b} = 0$, $U_{\beta_t} = U_b$, and $\mathcal{K}' = \frac{1}{2}\mathcal{K}$, where \mathcal{K}' is the mean atomic weight of the plasma. Making these substitutions into (35) and (60) with no U_{β_s} gives:

$$v_i = \sqrt{\frac{2(U_b + U_{\beta_t})}{M}} = \sqrt{\frac{2(2U_b)}{M}} \approx \sqrt{\frac{4U_b}{M}} = \sqrt{\frac{6RT}{\mathcal{K}'}} = \sqrt{\frac{6RT}{\mathcal{K}/2}} = \sqrt{\frac{12RT}{\mathcal{K}}} = 2\sqrt{\frac{3RT}{\mathcal{K}}} \quad (62)$$

The added $U_{\beta_t} = U_b$ gives twice the old value of v_i from (35); more generally, added U_{β_t} gives a linear increase in v_i and we can expect the same for r_e . This all means that for thermal plasmas, (40) is better expressed using the nucleon kinetic energy alone:

$$H_G = K \frac{\left(\frac{U_b + U_{\beta_t}}{U_b}\right)v_i}{\left(\frac{U_b + U_{\beta_t}}{U_b}\right)r_e} = K \frac{\sqrt{\frac{2U_b}{M}}}{r_e} \quad (63)$$

Where v_i and r_e have their non-ionized values. The mass partition $\rho' = 0.84$ is now folded into H_G . The denominator term associated with r_e in (63) is inserted to comply with the thermal model's zero-order dependencies. In (63), v_i remains close to (35): $U_b \approx 0.9995U_i$, so the effect of thermal ionization on H is minimal.

We proceed by assuming that suprathermal energy U_{β_s} has no effect on either K or r_e . It may have some effect but we will say it doesn't. Removal of U_{β_b} and U_{β_t} from (60) gives:

$$v_{i(b+\beta_s)} = \sqrt{\frac{2(U_b + U_{\beta_s})}{M}} = v_i \sqrt{\left(1 + \frac{U_{\beta_s}}{U_b}\right)} \quad (64)$$

Where $v_{i(b+\beta_s)}$ is the initial radial velocity of the light adiabatic sphere, v_i is the thermal value, and U_{β_s}/U_b is the

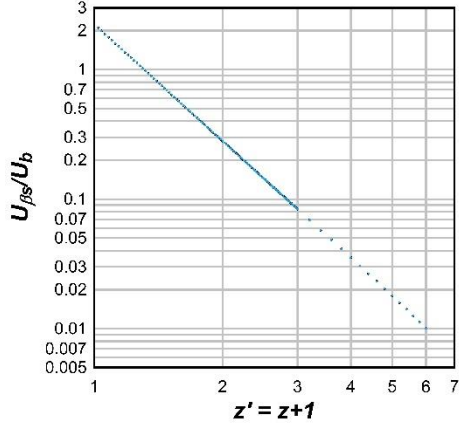


Figure 6. Suprathermal ratio vs. z'

suprathermal ratio.

Inserting (64) into (40) gives:

$$H = H_G \sqrt{\left(1 + \frac{U_{\beta_s}}{U_b}\right)} \quad (65)$$

Use of (63)-(64) to get (65) presupposes thermal plasma, a safe bet for a reionized Universe. We fit the light model (65) to the Λ CDM model (21) by convergence of U_{β_s}/U_b around $H/H_A = 1$ for each datum. To get H_G , we use ρ' (42) to get P_I in (26), giving r_e when $E_k = 0$, then getting thermal v_i from (35) and finally H_G from (40). The suprathermal ratio U_{β_s}/U_b is, like H_G , zero-order in T ,⁶ so (65) is completely temperature-independent. These results are shown in Figure 6. A ln-ln line is found⁷ for $z = 0 \rightarrow 2$, giving (66):

$$\frac{U_{\beta_s}}{U_b} = e^{(0.8045 - 2.9915 \ln(z'))} \approx \frac{2.236}{(z')^3} \quad (66)$$

At $z = 0$, $U_{\beta_s}/U_b = 2.2397$ gives $H/H_A = 1$; the regressed value is 2.236. This is close to the ratio $\Omega_\Lambda/(\Omega_b + \Omega_c)$ in the Λ CDM model, 2.235, and a simple restatement of the source of “dark energy” repulsion. At higher z , U_{β_s}/U_b drops steadily to 0.01 at $z = 5$. A modest deviance from linearity in the plot occurs above $z = 2$; these are shown in Figure 6 but not included in the regression. The crossover to U_{β_s} dominance is found at $z = 0.309$. Equation (66) derives from Λ CDM and accordingly gives the suprathermal ratio as proportionate to $(z')^{-3}$.

Using the same data, a ln-ln regression of r_e vs. z' gives (67):⁸

$$r_e = r_0 e^{[0.00006 - 1.5006 \ln(z')]} \approx r_0 (z')^{-\frac{3}{2}} \quad (67)$$

Where $r_0 = r_e$ at $z = 0$. From (67) we see that the adiabatic volume V_e/V_0 varies as $(z')^{-\frac{9}{2}}$, not $(z')^{-3}$. A constant “dark energy density” expressed as $[U_{\beta_s}/U_b]/(z')^3$ might be accurate, but within GCDM, isn’t proper.

From (65) – (67) we arrive at an expression of H for $z = 0$ to 2:

$$H = H_{G_0} z'^{\frac{3}{2}} \sqrt{1 + \frac{2.2397}{z'^3}} \quad (68)$$

⁶ $T = 4,000-50,000\text{K}$ gave the same results for all z .

⁷ For the ln-ln regression of $H(z)$ from $z = 0$ to 2, 101 data points were used with 3+ significant figures for all calculated U_{β_s}/U_b . Found: $y = 0.80455 - 2.99154x$; Correlation 0.9999996; std. error 0.0007. The y intercept gives $z = 0.30852$.

⁸ Found for ln-ln: $y = 0.00006 - 1.500563x$; correlation 0.99999999. The endpoint is temperature-dependent so a constant T must be used.

If $H_0 = 74.40$ km/sec/Mpc, then $H_{G_0} = 1.339 \times 10^{-18}$ sec $^{-1}$ is the thermal value at $z = 0$. The term $z' = z + 1$ is given by (19). Equation (68) gives 100.00% \rightarrow 99.90% of the Λ CDM value (21) for $z = 0$ to 2. The exponents in (66) – (68) are shown as rounded to the nearest fraction. The rounding excises CMB mass $\Delta m'$ (51) from r_e/r_0 (67) which may contribute to the observed -0.1% deviance at $z = 2$.

At $z = 0$, the models closely converge:

$$\frac{U_{\beta_s}}{(U_b + U_{\beta_s})} = \Omega_\Lambda = 0.691 \quad (69)$$

If we include thermal electrons in the denominator of (69), we get $\frac{U_{\beta_s}}{(U_b + U_{\beta_s} + U_{\beta_t})} = 0.53$, still more than half of all kinetic energy in the IGM today.

If one considers that U_{β_s} may persist indefinitely then a “pumped Universe” scenario is plausible. In a pumped Universe, suprathermal energy in the IGM accumulates. If U_{β_s} persists, then $d(U_{\beta_s})/dt$ can be estimated through lookback dz/dt at a constant T and compared to known E_γ sources: Type “O” stars, active galactic nuclei, etc. A constant $[U_{\beta_s}/U_b]/(z')^3$ should result for $z = 0$ to 2. Those calculations are more involved and lie outside the scope of the present paper.

4.2.1 Origin of suprathermal electrons in the IGM

By $z \approx 6$ the Universe was fully reionized, so Compton scattering from neutral IGM atoms isn't a significant source of suprathermal energy after that. A second source is Compton scattering of free electrons in the IGM, which would taper off to a steady state if the energy profiles of the electrons and photons were to converge. Cosmic radiation U_{b_s} from the web is a third source. The reader is asked to consider a fourth source, electron escape from the web, as a present-day contributor to the IGM's suprathermal content. Electrons move faster than protons, and any resulting IGM charge buildup is presently untreated. This author estimates these electrostatic effects as minor compared to U_{β_s} .

4.2.2 Suprathermal effects on r_e , K , and K_S

Suprathermal electrons do not obey the gas laws which underpin the thermal model. Many thermal electrons may not either as they can travel at relativistic speeds when hot enough. I can't offer much insight here; all we can say with certainty is that for a given U_{i_s} , ΔU_{i_s} isn't found from (15). The presumption that r_e and K are unaffected by U_{i_s} is purely conjectural, necessary for development of (65) – (69). Equation (68) does give the same results as (21), so whatever the suprathermal ratio actually describes, it works well. For special effects, the thermal model's r_e dependence follows (47); relativistic mass increase would cause a decrease in r_e . The entropic partition K_S and $v/v_i = K$ may also change with introduction of highly relativistic kinetic energy. Any such effects on (K/r_e) would be reflected at $z = 0$ giving $U_{\beta_s}/U_b - \Omega_\Lambda/\Omega_{(b+c)} > 0$. This happens to be true but the difference is small, about 0.2%, so I believe such changes in K and r_e aren't large. Even if (K/r_e) is theoretically shown to change by as much as 1%, the light model still allows us to use known and conserved energy sources, in compliance with (1), to account for H .

5 DISCUSSION: GCDM VERSUS Λ CDM

The Λ CDM model is a benchmark, giving the most accurate empirical fit to date. It closely converges with the GCDM model at $z = 0$. The models have different theoretical foundations and their predictions diverge at last scatter.

The Λ CDM model (21) combines three formulas:

- 1) The Friedmann equation gives a relation between H and rest energy density $\epsilon_{(b+c)}$.
- 2) The fluid equation adds a term “ P ” and describes covariant ($\epsilon_{(b+c)} + “P”$) vs. H .
- 3) The equation of state divides “ P ” into three different constituents.

We use $H(t)$ below. It’s connected to $H(a)$ in (21) by lookback $\int (dt/da) da$.

5.1 The Friedmann equation

The question of Universal curvature is historically important and extensively treated in modern texts [34-35]. That debate is largely settled now. Most of us believe in a flat Universe, so the Friedmann equation can be simply expressed:

$$H^2 = \frac{8\pi G \epsilon_{(b+c)}}{3c^2} \approx \frac{8\pi G \rho}{3} \quad (70)$$

In (70), ρ doesn’t include the equivalent mass of kinetic energy density ϵ_{U_i} , hence the “ \approx ”. Equation (70) in its Newtonian form ρ describes what happens when a model sphere of rocks within CDM expands in Euclidean space. The rocks and CDM have a primordial E_k which diminishes as they work against gravity dU . If CDM has no internal kinetic energy then the rocks do all the work.

Both models use the critical density (22) as a key parameter. The Λ CDM model uses $\epsilon(z) = \epsilon_{crit}$. It’s a flat fulcrum between a positively curved Universe, where the rocks slow down too much and end up collapsing, vs. a negatively curved Universe, where the rocks possess $E_k \gg 0$ forever. At the fulcrum, the rocks’ E_k is exactly spent by work, and $E_k \rightarrow 0$ asymptotically at infinite time. The word “critical” in “critical density” reflects this seemingly miraculous knife-edge balance. The GCDM model uses $\rho(z) = \rho_{crit}$. Its value reflects the perpetual 2:1 dominance of IGM gain $d(E_S)$ over total dU . The critical density is simply and exactly a monotonic consequence of the progress of entropy and time (2)-(3).

The Friedmann equation (70) underestimates E_k arising from P_V at higher z . This is most evident at last scatter: Atomic radial movement of the gas’s acoustic oscillation is ironically treated as nongaseous. This neglects the positive effect of CMB energy on the gas’s instant pressure. The CMB’s equivalent mass reduces the endpoint, shrinks the adiabatic sphere, and increases the baryon density. The resulting increase in instant pressure is proposed as the cause of the Hubble tension (Figure 4). When CMB energy is removed from the thermal model, H_G/H_A at last scatter drops from 1.25 to 0.95.

The acoustic oscillation calculations underlying the last-scatter H_A value derive in part from (70). Friedmann in turn derived (70) using general relativity which neglects entropic gain. Einstein’s field equation has no provision for this gain. Einstein added Λ to the field equation to offset the noncomoving or “static” model of the Universe then prevalent. The concept of Λ fell out of favor due in part to its unbound static instability. The contemporaneous 1917 observations of Vesto Slipher [40], followed later by Edwin Hubble in 1929 [41], then by Penzias and Wilson in 1965 [1] all led to a comoving model. Within this comoving model, Λ was reinserted, as it was then consistent with the model, and Einstein was Einstein. The value of Ω_Λ , however, was long thought to be zero. In 1998, two groups of researchers [36-39] gave Ω_Λ a nonzero value, 0.69, as this was consistent with their observations. Our Universe became filled with mysterious repulsive energy.

Einstein’s Λ was a proper addition to the field equation in 1917. It kept a “balloon” inflated in a static Universe. Einstein, along with the authors of [36-39], didn’t consider the possibility of gas pressure as a repulsive force. The baryon content of the IGM wasn’t estimated until well after 1917.

At very low redshifts, the CMB's Ω_λ in the "CDM-only" (41) is negligible and (41) \equiv (70). The Friedmann equation and the thermal model (53) give near-identical results from $z = 0$ to 10 (figure 5). The remaining differences between the Λ CDM and light models emerge from the fluid and acceleration equations, our next subject.

5.2 The fluid and acceleration equations

If all the energy in the Universe was CDM and accreted mass, its expansion would follow (70). CMB photons also have energy and mass equivalence which drops off faster than that of nonrelativistic mass. To reconcile these differing rates, the fluid equation (74) was devised. Its derivation starts with (71), the engineer's preferred expression of (1), describing gas in a bound vessel:

$$dE = TdS - PdV \quad (71)$$

Where $dE = d(U_i)$ is thermal change in the vessel. Also in this vessel,

$$dQ = TdS \quad (72)$$

Where dQ is heat flow to or from the vessel. A restriction is placed on (72), $dQ = 0$. So far, so good: The system is adiabatic, like the Universe. If $dQ = 0$ in (72), then $dS = 0$ as well. This precept is used to set dS in (71) to 0. A vessel's boundary is required for (72). A vessel isn't required for (71), but if dS in (71) is differentiated over time, an entropic term TdS/dt arises which at scale shouldn't be set to zero since that is inconsistent with the second law (2). This issue is skirted by removal of (71)'s TdS prior to time differentiation, giving:

$$PdV/dt = -dE/dt \quad (73)$$

Equation (73) is an isoentropic special case of (71) which describes the rate of thermal energy leaving an adiabatic vessel and performing work (e.g. dU). This is suitable for a bound system. When the "vessel" is the unbound Universe, (73) means that thermal loss in excess of dU is *leaving the Universe*. Absent any additional dimensions, or perhaps a Λ field which acquires the energy, that is not a conclusion to which this author can subscribe. Isoentropy, i.e. neglect of (2), leads to inconsistency with (1). If you neglect the second law, you are going to violate the first law. Insofar as Λ is concerned, energy is purported to come from it, not add to it. The consistent destination for any unbound thermal loss not taken up by gravity is $d(TS)$, giving $P_{V'}$ from (4) and (12), and E_k from (4) and (10). At scale, in (71) it's dE that's zero, not dS .

Equation (73) is used to derive the fluid equation (74), which redefines pressure $P \rightarrow "P"$:

$$\frac{d\epsilon_{(b+c)}}{dt} + 3H(\epsilon_{(b+c)} + "P") = 0 \quad (74)$$

The terms P and " P " are both expressed as J/m^3 , but " P " takes on a different meaning: Equivalent mass density. This redefinition cleared the way for inclusion of relativistic energy as one of " P "'s mass equivalent components. However, the repulsive nature of unbound $P (= P_{V'})$ is expunged since entropic gain TdS has been excised. The term " $P_{V'}$ " now means only the differential change in equivalent mass density arising from thermal loss $-d(\epsilon_{U_{it}})$. All of $\epsilon_{U_{it}}$ lies within " P " and is so small as to be practically nonexistent within (74).

The Newtonian expression of (74) is:

$$\frac{d\rho}{dt} + 3H(\rho_{(b+c)} + "P"/c^2) = 0 \quad (75)$$

Equation (75) better shows why thermal energy density is thought to be insignificant. Its equivalent mass density $\rho_{U_{it}} = \epsilon_{U_{it}}/c^2$ is dwarfed by the rest density of either the comoving atoms ρ_b or cold dark matter ρ_c .

The Friedmann equation (70) is differentiated and combined with (74) to give the acceleration equation (76):

$$\frac{dH}{dt} = - \left[\frac{4\pi G}{c^2} (\epsilon_{(b+c)} + "P") \right] = \frac{-4\pi G \epsilon_{M'}}{c^2} = -4\pi G \rho_{M'} \quad (76)$$

In Λ CDM, total and critical densities are the same thing: $\epsilon_{M'} = \epsilon_{crit}$. Equation (76), like its progenitor (70), treats all mass as accreted, so (76) doesn't properly express entropic $P_{V'}$. Partly neglected by (70), $P_{V'}$ is then excised altogether by (74). The repulsive effects of the suprathermal portion of $P_{V'}$ are instead expressed by Einstein's resurrected Λ , whose attendant density ($-\epsilon_A$) is added to "P".

The expressions in (76) are arbitrarily parsed and better seen as a sum of densities, now including $-\epsilon_A$:

$$\frac{dH}{dt} = \frac{-4\pi G \epsilon_{M'}}{c^2} = \frac{-4\pi G}{c^2} [\epsilon_b + \epsilon_c + \epsilon_{CMB} + \epsilon_{U_i} + \epsilon_\gamma + \epsilon_{E_i} - \epsilon_A] \quad (77)$$

Where ϵ_γ is emitted photons and ϵ_{E_i} is ionization. In GCDM, ϵ_A doesn't exist, and $\epsilon_{M'}$ is:

$$\epsilon_{M'} = (\epsilon_b + \epsilon_c + \epsilon_{CMB} + \epsilon_{U_i} + \epsilon_\gamma + \epsilon_{E_i}) \approx \epsilon_b + \epsilon_c + \epsilon_{CMB} \quad (78)$$

At last scatter, relativistic mass from the CMB was important: $\epsilon_{CMB} = 0.24\epsilon_{M'}$. By $z = 9$ it was only $0.003\epsilon_{M'}$. That was more than ten billion years ago. Today at $z = 0$, the GCDM model gives CMB energy as $0.0003\epsilon_{M'}$. If we make an ad hoc 1% allowance for special effects and the remainders $\epsilon_\gamma + \epsilon_{U_i} + \epsilon_{E_i}$, then rest density $\rho_{(b+c)}$ can be seen as 99% of $\epsilon_{M'}/c^2$ for most of the Universe's history. Baryons behave as an 84% unbound gas with unchanged rest mass, whose replenished thermal loss drives expansion through entropic gain. The spacetime curvatures from stars and galaxies in the cosmic web are only local perturbations in a much more voluminous, massive, and Euclidean IGM.

The instant IGM is, I contend, effectively Euclidean. Equivalent mass density $\rho_{M'}$ was scalar in xyz at last scatter, so U was too, and it remained so in the IGM during and after accretion. The IGM's density ρ over all $z = 0 \rightarrow 1089$ is so low, and its mass fraction ρ' so large, that particle movement within can be fairly described using Euclidean momentum tensors in a covariant scalar U field. Add up the tensors' kinetic energy, and you get U_i . Progress of time in the IGM is linear for this entire z range: clocks at $z = 0$ and 1089 differ by less than a year in a million. A flat instant Universe ought to be Euclidean *ad infinitum*,⁹ which is consistent with the IGM's treatment as such.

GCDM's suprathermal pressure $P_{V_s'} \equiv \epsilon_{U_{i_s}}$ is expressed within Λ CDM by $-\epsilon_A$, whose 0.69 dominance of ϵ_{crit} at $z = 0$ arises from another inconsistency: Conflation.

Conflation of meaning between thermal and rest energies in (71) and (73) contributes to Λ CDM's theoretical inconsistency. A single symbol, E , is used to describe them behaving the same way. They don't. The fluid equation (74) is derived from a thermal law (71) and treats rest energy $E = Mc^2$ as thermally variable. It isn't. Rest mass M is constant (27) and no more related to thermal change than the Mc^2 of a pendulum is to its apogee. The fluid equation's improper inclusion of these enormous amounts of variable and fictitious rest energy into what is properly minor thermal change gives substantial inconsistency with (1) and alters every downstream calculation. This is why Λ CDM's $\Omega_\Lambda = \epsilon_A/\epsilon_{crit} = 0.69$ is found to be so large today [36-39]. Such "dark energy" arises because

⁹ This concept of an instant Euclidean Universe can be extended all the way back to the end of the inflationary period, when the v_i of an adiabatic sphere fell below c .

$dE \neq 0$ in (71). If energy is conserved and entropy gained, then the observed stellar movement attributed to $-\epsilon_A$ is more properly expressed as arising from $+P_{V_s}'$.

The Jeans model of star formation [25] is relevant to our discussion here. At last scatter, both (76) and the Jeans model operated concurrently within any given volume. The Jeans model treats P as repulsive, an offset against gravitational collapse. The acceleration equation (76) treats “ P ” as attractive and is inconsistent with the Jeans model. The Λ CDM model treats P as repulsive, which is consistent with the Jeans model’s treatment of P .

5.3 The equation of state

The Λ CDM equation of state (79) describes the components comprising “pressure P ” and has three terms: baryonic, relativistic, and Λ :

$$"P" = w_b \epsilon_b + w_\lambda \epsilon_\lambda + w_\Lambda \epsilon_\Lambda \quad (79)$$

The w terms are dimensionless numbers: $w_b \ll 1$, $w_\lambda = 1/3$, and $w_\Lambda = -1$. Equation (79) is combined with (76) to complete the Λ CDM model (21).

5.3.1 Baryonic mass

Baryonic matter comprises stars, rocks, and helium balloons, and is treated by Λ CDM as 100% attractive. This might disturb a vendor watching his balloons implode. In GCDM, baryon mass is mostly repulsive, a gas: The balloon vendor feels better. At last scatter, baryon mass was 100% gas: Helium and H_1 . Presently, the repulsive : attractive ratio of baryon mass in the Universe is about $5\frac{1}{4} : 1$.

The Λ CDM term $w_b \epsilon_b$ is expressed as:

$$w_b \epsilon_b \approx \left(\frac{kT}{\mu c^2} \right) \epsilon_b = \left(\frac{kT}{\mu c^2} \right) (\rho_b c^2) = \frac{kT \rho_b}{\mu} \quad (80)$$

Where μ is the mean atomic mass and k is Boltzmann’s constant. Equations (80) and (16) give the same thermal kinetic energy density $\epsilon_{U_{it}} = \frac{3}{2} P_{V_t}'$. This is negligible compared to ϵ_{crit} , as is suprathermal pressure P_{V_s}' which is instead treated by Λ CDM (21) as the conflated term Ω_A . In GCDM, there is no Ω_A , and P_{V_t}' provides both thermal and suprathermal repulsive force.

5.3.2 Relativistic mass; entropy of a photon

Relativistic mass, expressed as $w_\lambda \epsilon_\lambda$ in the Λ CDM model, is attractive in both models and arises from photon and neutrino energy.¹⁰ However, relativistic mass has opposite effects on the models’ behavior. In Λ CDM, H is reduced by added relativistic mass. In GCDM, H is increased, as relativistic mass’ gravitational pull increases baryon density and thus its instant pressure. Instant pressure always exceeds differential gravity loss by at least 2:1 (figure 3), so the more dense the gas becomes, the faster it expands. Of course, at some sufficiently large density, antinode formation from acoustic resonance causes collapse into accreted bodies, but at the low densities in the regions of the Universe that we have examined in the present paper, this is not something we need to worry about.

We now examine photon energy more closely. An expanding sphere of CMB light has an r^{-4} dependence of energy density. Volume increases as r^3 , so there appears to be a $1/r$ loss of CMB energy upon expansion. During the dark age there was minimal CMB energy transfer to the IGM’s baryons [29]. Most of the CMB’s energy vanished; we

¹⁰ Neutrinos are believed to have had relativistic kinetic energy at last scatter but became nonrelativistic in the dark age. This affects their temporal mass density dependence, which is untreated in the present paper.

get inconsistency with (1). I see no escape from this conundrum except to apply (3): CMB light yields gain through wavelength stretch $\Delta\lambda$. Any one CMB photon's wavelength increases with time and their combined lost energy is gain $\Delta E_{S_{\Delta\lambda}}$:

$$\Delta E_{S_{\Delta\lambda}} = E_{CMB_1} - E_{CMB_2} = \sum_{\lambda_1 \approx 0}^{\infty} n_{\lambda} h c \left(\frac{1}{\lambda_1} - \frac{1}{\lambda_2} \right) \quad (81)$$

where E_{CMB_1} and E_{CMB_2} are the before and after photon energies during the dark age, h is Planck's constant, λ_1 and λ_2 are the before and after wavelengths of the stretched photon, and n_{λ} is the number of photons at a wavelength λ_1 . The distribution n_{λ} vs. λ is observed in the CMB as a blackbody curve, and extrapolated to give n_{λ} vs. λ_1 at last scatter.

The above analysis gives an individual photon's entropy S_{λ} as equal to Planck's constant:

$$S_{\lambda} = h \quad (82)$$

Entropy is expressed as J/Hz rather than the more conventional J/K.¹¹ Unbound photon energy E_{λ} is potentially 100% entropic, in that all of it is eventually lost to time.

During the dark age $E_{\lambda} = E_{CMB}$ and the photon energy density $\epsilon_{\lambda} = \frac{E_{\lambda}}{V}$ followed (83):

$$\epsilon_{\lambda} = \int_{f=0}^{\infty} \frac{n_f h f}{V} = 7.566 * 10^{-16} T^4 \quad (83)$$

Where n_f is the number of photons of frequency f at a given blackbody T . After stars began to flood the Universe with photon energy E_{γ} , $E_{\lambda} = (E_{CMB} + E_{\gamma})$. Photons E_{γ} also stretch and gain.

From (82), photons are isoentropic, so the second law as applied to them is expressed with gain (3) rather than simple entropy increase (2). Gain $d(E_S)$ is connected to E_k (10), hence volume (13). The rate of volume increase dV_{λ}/dt of radial light in a model sphere is:

$$\frac{dV_{\lambda}}{dt} = \frac{4\pi c^3}{3} \quad (84)$$

which far outpaces nonrelativistic E_k .

Current treatment of CMB energy also begins isoentropically (73). While the present paper concurs with isoentropic photon treatment, photon gain $\Delta E_{S_{\Delta\lambda}}$ is neglected, and light energy is purported to expand more slowly than baryonic matter. A different result might be found if $\Delta E_{S_{\Delta\lambda}}$ is included in an *ab initio* derivation. In the observable Universe, $\Delta E_{S_{\Delta\lambda}}$ may affect H at $z \approx 1089$, as free electrons were still present at $z > 1089$ along with residual ionizing radiation, and photons were more strongly coupled to baryon movement.

Free electron gain at scale resembles that of photons as it's also a function of wavelength.

5.3.3 Dark energy

The remaining term, $w_{\Lambda}\epsilon_{\Lambda}$, describes repulsion. In the Λ CDM model, Λ is used to account for the behavior of stars in the more recent Universe, e.g. [36-39]. The term $w_{\Lambda} = -1$ arises because (79) treats “ P ” as attractive, so $w_{\Lambda}\epsilon_{\Lambda}$ has to have negative “pressure”. Its predominance, $\epsilon_{\Lambda} = 0.69\epsilon_{crit}$ at $z = 0$, arises from (74)'s dual inconsistencies of isoentropic expansion and variable rest energy. In the GCDM model, expansion is entropic, rest mass is constant,

¹¹ An alternate treatment of photon entropy using J/K instead of J/Hz is given by Kirwan [42].

and the behavior described by $w_A \epsilon_A$ arises from suprathermal pressure P_{V_s} in the IGM, mostly carried by electrons. These electrons do create a repulsive *in toto* scalar field, but unlike Λ its value is covariant and can be locally nonscalar. A noncovariant Λ means a constant ϵ_A . This creates more and more energy over time, which is inconsistent with (1). If (1) is obeyed, the field must be able to acquire energy from a conserved source. Suprathermal energy U_{i_s} meets this requirement.

6 CONCLUSIONS

The present paper proposes a fundamental change in the way the Universe is viewed: As an unbound thermodynamic system in which a freely expanding gas has partly coalesced into stars. A model which adheres to the second law of thermodynamics is achieved through the gas laws at last scatter and applied to the more recent plasmonic Universe. The Universe contains a repulsive field, IGM kinetic energy, scalar in xyz at last scatter. It's now locally variable in xyz but still behaves *in toto* as a covariant scalar in the flat Universe we see. The IGM's kinetic energy field has both thermal and suprathermal components; the former gives the Hubble tension and the latter causes "dark energy" Λ .

There are presently considered to be four fundamental forces of Nature: Strong, weak, electromagnetic, and gravitational. Entropic force should be added to this list. It can't be derived from the other four forces, it pushes apart distant galaxies, and it keeps a child's birthday balloon inflated. Entropic force operates over a wide range of scale. The balloon, and child, give us perspective.

DATA AVAILABILITY

An annotated .XLSX workbook containing the model and its output is available from the author. It has easy, step-by-step instructions for the interested reader.

References

- [1] Arno A. Penzias & Robert W. Wilson. (1965). A measurement of excess antenna temperature at 4080 Mc/s. *Astrophys. J.* 142, 419-421. <https://adsabs.harvard.edu/full/1965ApJ...142..419P/0000419.000.html>
- [2] Philip Bull et al. (2016). Beyond Λ CDM: Problems, solutions, and the road ahead. *Phys. Dark. Univ.* 12, 56-99. <https://doi.org/10.1016/j.dark.2016.02.001>
- [3] Cormac O'Raiheartaigh, Michael O'Keefe, Werner Nahm, & Simon Mitton. (2017). Einstein's 1917 static model of the universe: a centennial review. *Eur. Phys. J. H* 42, 431-474. <https://doi.org/10.1140/epjh/e2017-80002-5>
- [4] D. Scolnic et al. (2014). Systematic uncertainties associated with the cosmological analysis of the first pan-starrs1 type Ia supernova sample. *Astrophys. J.* 795, 45. <https://doi.org/10.1088/0004-637X/795/1/45>
- [5] Adam G. Riess et al. (2018). New parallaxes of galactic cepheids from spatially scanning the Hubble space telescope: Implications for the Hubble constant. *Astrophys. J.* 855, 136. <https://doi.org/10.3847/1538-4357/aaadb7>
- [6] Adam G. Riess, Stefano Casertano, Wenlong Yuan, Lucas M. Macri, & Dan Scolnic. (2019). Large Magellanic cloud cepheid standards provide a 1% foundation for the determination of the Hubble constant and stronger evidence for physics beyond Λ CDM. *Astrophys. J.* 876, 85. <https://doi.org/10.3847/1538-4357/ab1422>

- [7] Licia Verde, Tommaso Treu, & Adam G. Riess. (2019) Tensions between the early and late Universe. *Nat. Astron.* 3, 891-895. <https://doi.org/10.1038/s41550-019-0902-0>
- [8] A. J. Shajib et al. (2020). STRIDES: a 3.9 per cent measurement of the Hubble constant from the strong lens system DES J0408–5354. *MNRAS* 494, 6072-6102 <https://doi.org/10.1093/mnras/staa828>
- [9] Kenneth C. Wong et al. (2020). H0LiCOW – XIII. A 2.4 per cent measurement of H_0 from lensed quasars: 5.3σ tension between early- and late-Universe probes. *MNRAS* 498, 1420-1439. <https://doi.org/10.1093/mnras/stz3094>
- [10] Vivian Poulin, Tristan L. Smith, Tanvi Karwal & Marc Kamionkowski. (2019). Early dark energy can resolve the Hubble tension. *Phys. Rev. Lett.* 122, 221301. <https://doi.org/10.1103/PhysRevLett.122.221301>
- [11] Nils Schöneberg, Julien Lesgourges, & Deanna C. Hooper. (2019). The BAO+BBN take on the Hubble tension. *J. Cosmol. Astroparticle Phys.* 2019, 10, 029. <https://doi.org/10.1088/1475-7516/2019/10/029>
- [12] Charles L. Steinhardt, Albert Sneppen, & Bidisha Sen. (2020). Effects of supernova redshift uncertainties on the determination of cosmological parameters. *Astrophys. J.* 902, 14. <https://doi.org/10.3847/1538-4357/abb140>
- [13] George Alestas & Leandros Perivolaropoulos. (2021). Late-time approaches to the Hubble tension deforming $H(z)$, worsen the growth tension. *MNRAS* 504, 3956-3962. <https://doi.org/10.1093/mnras/stab1070>
- [14] Eleonora Di Valentino et al. (2021). In the realm of the Hubble tension—a review of solutions. *Classical and Quantum Gravity* 38, 153001. <https://doi.org/10.1088/1361-6382/ac086d>
- [15] C. Krishnan, E. Ó Colgáin, M. M. Sheikh-Jabbari & Tao Yang. (2021). Running Hubble tension and a H_0 diagnostic. *Phys. Rev. D* 103, 10, 103509. <https://doi.org/10.1103/PhysRevD.103.103509>
- [16] Mohamed Rameez & Subir Sarkar. (2021). Is there really a Hubble tension? *Classical and Quantum Gravity* 38, 154005 <https://doi.org/10.1088/1361-6382/ac0f39>
- [17] Daniel Aloni, Asher Berlin, Melissa Joseph, Martin Schmaltz & Neal Weiner. (2022). A Step in understanding the Hubble tension. *Phys. Rev. D.* 105, 12, 123516. <https://doi.org/10.1103/PhysRevD.105.123516>
- [18] L. Perivolaropoulos & F. Skara. (2022). Challenges for Λ CDM: An update. *New Astron. Rev.* 95, 101659. <https://doi.org/10.1016/j.newar.2022.101659>
- [19] Naser Mostaghel. (2022). The source of tension in the measurements of the Hubble constant. *Int. J. Astron. Astrophys.* 12, 3, 273-280. <https://doi.org/10.4236/ijaa.2022.123016>
- [20] Vladimir Netchitailo. (2022). Hubble tension. *JHEPGC* 8, 2, 392-401 <https://doi.org/10.4236/jhepgc.2022.82030>
- [21] Shinji Tsujikawa. (2013). Quintessence: a review. *Classical and Quantum Gravity* 30, 214003. <https://doi.org/10.1088/0264-9381/30/21/214003>
- [22] Erik Verlinde. (2011). On the origin of gravity and the laws of Newton. *J. High Energy Phys.* 2011, 4, 20 [https://doi.org/10.1007/JHEP04\(2011\)029](https://doi.org/10.1007/JHEP04(2011)029)
- [23] Steven Weinberg. (1988). *The First Three Minutes*, Basic Books Press.

- [24] Planck Collaboration. (2020). Planck 2018 results. *A&A* 641, A1 <https://doi.org/10.1051/0004-6361/201833880>
- [25] J. Michael Owen & Jens V. Villumsen. (1997). Baryons, dark matter, and the Jeans mass in simulations of cosmological structure formation. *Astrophys. J.* 481, 1, 1-21. <https://doi.org/10.1086/304018>
- [26] Jordi Miralda-Escude. (2003). The dark age of the Universe. *Science* 300, 5267, 1904-1909. <https://doi.org/10.1126/science.1085325>
- [27] Aravind Natarajan & Naoki Yoshida. (2014). The dark ages of the Universe and hydrogen reionization. *Prog. Theor. Exp. Phys.* 2014, 06B112 <https://doi.org/10.1093/ptep/ptu067>
- [28] Gianfranco Bertone & Dan Hooper. (2018). History of dark matter. *Rev. Mod. Phys.* 90, 045002. <https://doi.org/10.1103/RevModPhys.90.045002>
- [29] Tejaswi Venumadhav, Liang Dai, Alexander Kaurov & Matias Zaldarriaga. (2018). Heating of the intergalactic medium by the cosmic microwave background during cosmic dawn. *Phys. Rev. D* 98, 10, 103513. <https://doi.org/10.1103/PhysRevD.98.103513>
- [30] B. E. Robertson et al. (2023). Identification and properties of intense star-forming galaxies at redshifts $z > 10$. *Nat. Astron.* 7, 5, 611-621 <https://doi.org/10.1038/s41550-023-01921-1>
- [31] Emma Curtis-Lake et al. (2023). Spectroscopic confirmation of four metal-poor galaxies at $z = 10.3-13.2$. *Nat. Astron.* 7, 5, 622-632. <https://doi.org/10.1038/s41550-023-01918-w>
- [32] Hasan Yüksel, Matthew D. Kistler, John F. Beacom, & Andrew M. Hopkins. (2008). Revealing the high-redshift star formation rate with gamma-ray bursts. *Astrophys. J.* 683, 1, L5. <https://doi.org/10.1086/591449>
- [33] David Wanderman & Tsvi Piran. (2010). The luminosity function and the rate of Swift's gamma-ray bursts. *MNRAS* 406, 3, 1944-1958. <https://dx.doi.org/10.1111/j.1365-2966.2010.16787.x>
- [34] Andrew Liddle. (2015). *An introduction to modern cosmology*, Wiley. ISBN 978-1-118-50214-3.
- [35] Barbara Ryden. (2017). *Introduction to cosmology, second edition*. Cambridge University Press. <https://www.cambridge.org/9781107154834>.
- [36] Saul Perlmutter et al. (1998). Discovery of a supernova explosion at half the age of the Universe. *Nature* 391, 51-54. <https://doi.org/10.1038/34124>
- [37] Saul Perlmutter et al. (1999). Measurements of Ω and Λ from 42 high-redshift supernovae. *Astrophys. J.* 517, 2, 565-586. <https://doi.org/10.1086/307221>
- [38] Adam G. Riess et al. (1998). Observational evidence from supernovae for an accelerating Universe and a cosmological constant. *Astron. J.* 116, 3, 1009. <https://doi.org/10.1086/300499>
- [39] Adam G. Riess et al. (2004). Type Ia supernova discoveries at $z > 1$ from the Hubble space telescope: Evidence for past deceleration and constraints on dark energy evolution. *Astrophys. J.* 607, 2, 665. <https://doi.org/10.1086/383612>
- [40] Vesto M. Slipher. (1917). Radial velocity observations of spiral nebulae. *The Observatory* 40, 304-306. <https://ui.adsabs.harvard.edu/abs/1917Obs...40..304S/abstract>
- [41] Edwin Hubble. (1929). A relation between distance and radial velocity among extra-galactic nebulae. *Proc. Nat. Acad. Sci.* 15, 3, 168-173. <https://doi.org/10.1073/pnas.15.3.168>

- [42] A. D. Kirwan Jr. (2004). Intrinsic photon entropy? The darkside of light. *Int. J. Eng. Sci.* 42, 7, 725-734.
<https://doi.org/10.1016/j.ijengsci.2003.09.005>